

Comparison of pp and $p\bar{p}$ differential elastic cross sections and observation of the exchange of a colorless C -odd gluonic compound

V.M. Abazov^{†,47} B. Abbott^{†,90} B.S. Acharya^{†,33} M. Adams^{†,68} T. Adams^{†,66} J.P. Agnew^{†,62} G.D. Alexeev^{†,47}
G. Alkhazov^{†,52} A. Alton^{a†,78} G. Antchev^{†,4} A. Askew^{†,66} P. Aspell^{†,57} I. Atanassov^{†,4} S. Atkins^{†,76} K. Augsten^{†,9}
V. Aushev^{†,59} Y. Aushev^{†,59} V. Avati^{†,46,57} C. Avila^{†,6} F. Badaud^{†,14} J. Baechler^{†,57} L. Bagby^{†,67}
C. Baldenegro Barrera^{†,75} B. Baldin^{†,67} D.V. Bandurin^{†,97} S. Banerjee^{†,33} E. Barberis^{†,77} P. Baringer^{†,75}
J.F. Bartlett^{†,67} U. Basser^{†,19} V. Bazterra^{†,68} A. Bean^{†,75} M. Begalli^{†,2} L. Bellantoni^{†,67} V. Berardi^{†,35,36}
S.B. Beri^{†,31} G. Bernardi^{†,18} R. Bernhard^{†,23} M. Berretti^{†,12} I. Bertram^{†,60} M. Besançon^{†,19} R. Beuselinck^{†,61}
P.C. Bhat^{†,67} S. Bhatia^{†,80} V. Bhatnagar^{†,31} G. Blazey^{†,69} S. Blessing^{†,66} K. Bloom^{†,81} A. Boehnlein^{†,67}
D. Boline^{†,86} E.E. Boos^{†,49} V. Borchsh^{†,53} G. Borissov^{†,60} M. Borysova^{†,59} E. Bossini^{†,41,57} U. Bottigli^{†,41}
M. Bozzo^{†,38,39} A. Brandt^{†,94} O. Brandt^{†,24} M. Brochmann^{†,98} R. Brock^{†,79} A. Bross^{†,67} D. Brown^{†,18}
X.B. Bu^{†,67} M. Buehler^{†,67} V. Buescher^{†,25} V. Bunichev^{†,49} S. Burdin^{b†,60} H. Burkhardt^{†,57} C.P. Buszello^{†,56}
F. S. Cafagna^{†,35} E. Camacho-Pérez^{†,43} B.C.K. Casey^{†,67} H. Castilla-Valdez^{†,43} M. G. Catanesi^{†,35}
S. Caughron^{†,79} S. Chakrabarti^{†,86} K.M. Chan^{†,73} A. Chandra^{†,96} E. Chapon^{†,19} G. Chen^{†,75} S.W. Cho^{†,42}
S. Choi^{†,42} B. Choudhary^{†,32} S. Cihangir^{†,67} D. Claes^{†,81} J. Clutter^{†,75} M. Cooke^{j†,67} W.E. Cooper^{†,67}
M. Corcoran^{†,96} F. Couderc^{†,19} M.-C. Cousinou^{†,16} M. Csanád^{†,29,27} T. Csörgö^{†,29,30} J. Cuth^{†,25} D. Cutts^{†,93}
A. Das^{†,95} G. Davies^{†,61} M. Deile^{†,57} S.J. de Jong^{†,44,45} E. De La Cruz-Burelo^{†,43} F. De Leonardis^{†,37,35}
F. Déliot^{†,19} R. Demina^{†,85} D. Denisov^{†,87} S.P. Denisov^{†,51} S. Desai^{†,67} C. Deterre^{c†,62} K. DeVaughan^{†,81}
H.T. Diehl^{†,67} M. Diesburg^{†,67} P.F. Ding^{†,62} A. Dominguez^{†,81} M. Doubek^{†,9} A. Drutskoy^{q†,48} D. Druzhkin^{†,53,57}
A. Dubey^{†,32} L.V. Dudko^{†,49} A. Duperrin^{†,16} S. Dutt^{†,31} M. Eads^{†,69} D. Edmunds^{†,79} K. Eggert^{†,88} J. Ellison^{†,64}
V.D. Elvira^{†,67} Y. Enari^{†,18} V. Eremin^{†,50} H. Evans^{†,71} A. Evdokimov^{†,68} V.N. Evdokimov^{†,51} A. Fauré^{†,19}
L. Feng^{†,69} T. Ferbel^{†,85} F. Ferro^{†,38} F. Fiedler^{†,25} A. Fiergolski^{†,57} F. Filthaut^{†,44,45} W. Fisher^{†,79}
H.E. Fisk^{†,67} L. Forthomme^{†,12,13} M. Fortner^{†,69} H. Fox^{†,60} J. Franc^{†,9} S. Fuess^{†,67} P.H. Garbincius^{†,67}
F. Garcia^{†,12} A. Garcia-Bellido^{†,85} J.A. García-González^{†,43} V. Gavrilov^{†,48} W. Geng^{†,16,79} V. Georgiev^{†,7}
C.E. Gerber^{†,68} Y. Gershtein^{†,82} S. Gianini^{†,57} G. Ginther^{†,67} O. Gogota^{†,59} G. Golovanov^{†,47} P.D. Grannis^{†,86}
S. Greder^{†,20} H. Greenlee^{†,67} G. Grenier^{†,21} Ph. Gris^{†,14} J.-F. Grivaz^{†,17} A. Grohsjean^{c†,19} S. Grünendahl^{†,67}
M.W. Grünewald^{†,34} L. Grzanka^{†,46} T. Guillemin^{†,17} G. Gutierrez^{†,67} P. Gutierrez^{†,90} J. Haley^{†,91}
J. Hammerbauer^{†,7} L. Han^{†,5} K. Harder^{†,62} A. Harel^{†,85} J.M. Hauptman^{†,74} J. Hays^{†,61} T. Head^{†,62}
T. Hebbeker^{†,22} D. Hedin^{†,69} H. Hegab^{†,91} A.P. Heinson^{†,64} U. Heintz^{†,93} C. Hensel^{†,1} I. Heredia-De La Cruz^{d†,43}
K. Herner^{†,67} G. Hesketh^{f†,62} M.D. Hildreth^{†,73} R. Hirosky^{†,97} T. Hoang^{†,66} J.D. Hobbs^{†,86} B. Hoeneisen^{†,11}
J. Hogan^{†,96} M. Hohlfield^{†,25} J.L. Holzbauer^{†,80} I. Howley^{†,94} Z. Hubacek^{†,9,19} V. Hynek^{†,9} I. Iashvili^{†,84}
Y. Ilchenko^{†,95} R. Illingworth^{†,67} T. Isidori^{†,75} A.S. Ito^{†,67} V. Ivanchenko^{†,53} S. Jabeen^{m†,67} M. Jaffré^{†,17}
M. Janda^{†,9} A. Jayasinghe^{†,90} M.S. Jeong^{†,42} R. Jesik^{†,61} P. Jiang^{†,5} K. Johns^{†,63} E. Johnson^{†,79} M. Johnson^{†,67}
A. Jonckheere^{†,67} P. Jonsson^{†,61} J. Joshi^{†,64} A.W. Jung^{o†,67} A. Juste^{†,54} E. Kajfasz^{†,16} A. Karev^{†,57}
D. Karmanov^{†,49} J. Kašpar^{†,10,57} I. Katsanos^{†,81} M. Kaur^{†,31} B. Kaynak^{†,58} R. Kehoe^{†,95} S. Kermiche^{†,16}
N. Khalatyan^{†,67} A. Khanov^{†,91} A. Kharchilava^{†,84} Y.N. Kharzheev^{†,47} I. Kiselevich^{†,48} J.M. Kohli^{†,31} J. Kopal^{†,57}
A.V. Kozelov^{†,51} J. Kraus^{†,80} A. Kumar^{†,84} V. Kundrát^{†,10} A. Kupco^{†,10} T. Kurča^{†,21} V.A. Kuzmin^{†,49}
S. Lami^{†,40} S. Lammers^{†,71} G. Latino^{†,41} P. Lebrun^{†,21} H.S. Lee^{†,42} S.W. Lee^{†,74} W.M. Lee^{†,67} X. Le^{†,63}
J. Lellouch^{†,18} D. Li^{†,18} H. Li^{†,97} L. Li^{†,64} Q.Z. Li^{†,67} J.K. Lim^{†,42} D. Lincoln^{†,67} C. Lindsey^{†,75} R. Linhart^{†,7}
J. Linnemann^{†,79} V.V. Lipaev^{†,51} R. Lipton^{†,67} H. Liu^{†,95} Y. Liu^{†,5} A. Lobodenko^{†,52} M. Lokajicek^{†,10}
M. V. Lokajíček^{†,10} R. Lopes de Sa^{†,67} L. Losurdo^{†,41} F. Lucas Rodríguez^{†,57} R. Luna-Garcia^{g†,43} A.L. Lyon^{†,67}
A.K.A. Maciel^{†,1} M. Macrì^{†,38} R. Madar^{†,23} R. Magaña-Villalba^{†,43} M. Malawski^{†,46} S. Malik^{†,81} V.L. Malyshev^{†,47}
J. Mansour^{†,24} J. Martínez-Ortega^{†,43} R. McCarthy^{†,86} C.L. McGivern^{†,62} M.M. Meijer^{†,44,45} A. Melnitchouk^{†,67}
D. Menezes^{†,69} P.G. Mercadante^{†,3} M. Merkin^{†,49} A. Meyer^{†,22} J. Meyer^{i†,24} F. Miconi^{†,20} N. Minafra^{†,75}
S. Minutoli^{†,38} N.K. Mondal^{†,33} M. Mulhearn^{†,97} T. Naaranoja^{†,12,13} E. Nagy^{†,16} M. Narain^{†,93} R. Nayyar^{†,63}
H.A. Neal^{†,78} J.P. Negret^{†,6} F. Nemes^{†,57,29} P. Neustroev^{†,52} H.T. Nguyen^{†,97} H. Niewiadomski^{†,88} T. Novák^{†,30}
T. Nunnemann^{†,26} E. Oliveri^{†,57} F. Oljemark^{†,12,13} J. Orduna^{†,93} M. Oriunno^{†,65} N. Osman^{†,16} K. Österberg^{†,12,13}
A. Pal^{†,94} P. Palazzi^{†,57} N. Parashar^{†,72} V. Parihar^{†,93} S.K. Park^{†,42} R. Partridge^{e†,93} N. Parua^{†,71}
R. Pasechnik^{†,55} V. Passaro^{†,37,35} A. Patwa^{j†,87} B. Penning^{†,61} M. Perfilov^{†,49} Z. Peroutka^{†,7} Y. Peters^{†,62}
K. Petridis^{†,62} G. Petrillo^{†,85} P. Pétroff^{†,17} M.-A. Pleier^{†,87} V.M. Podstavkov^{†,67} A.V. Popov^{†,51} M. Prewitt^{†,96}

D. Price^{†, 62} J. Procházka^{‡, 10} N. Prokopenko^{†, 51} J. Qian^{†, 78} A. Quadt^{†, 24} B. Quinn^{†, 80} M. Quinto^{‡, 35, 36}
T.G. Raben^{†, 75} E. Radermacher^{‡, 57} E. Radicioni^{‡, 35} P.N. Ratoff^{†, 60} F. Ravotti^{‡, 57} I. Razumov^{†, 51}
I. Ripp-Baudot^{†, 20} F. Rizatdinova^{†, 91} E. Robutti^{‡, 38} M. Rominsky^{†, 67} A. Ross^{†, 60} C. Royon^{†, 75} P. Rubinov^{†, 67}
R. Ruchti^{†, 73} G. Ruggiero^{‡, 57} H. Saarikko^{‡, 12, 13} G. Sajot^{†, 15} V.D. Samoylenko^{‡, 51} A. Sánchez-Hernández^{†, 43}
M.P. Sanders^{†, 26} A.S. Santos^{h†, 1} G. Savage^{†, 67} M. Savitskiy^{†, 59} L. Sawyer^{†, 76} T. Scanlon^{†, 61} R.D. Schamberger^{†, 86}
Y. Scheglov^{‡, 52} H. Schellman^{†, 92, 70} M. Schott^{†, 25} C. Schwanenberger^{c†, 62} R. Schwienhorst^{†, 79} A. Scribano^{‡, 40}
J. Sekaric^{†, 75} H. Severini^{†, 90} E. Shabalina^{†, 24} V. Shary^{†, 19} S. Shaw^{†, 62} A.A. Shchukin^{†, 51} O. Shkola^{†, 59}
V. Simak^{‡, 9} J. Siroky^{†, 7} P. Skubic^{†, 90} P. Slattey^{†, 85} J. Smajek^{‡, 57} W. Snoeys^{‡, 57} G.R. Snow^{‡, 81} J. Snow^{†, 89}
S. Snyder^{†, 87} S. Söldner-Rembold^{‡, 62} L. Sonnenschein^{†, 22} K. Soustruznik^{†, 8} J. Stark^{†, 15} N. Stefaniuk^{†, 59}
R. Stefanovitch^{‡, 57} A. Ster^{†, 29} D.A. Stoyanova^{†, 51} M. Strauss^{†, 90} L. Suter^{†, 62} P. Svoisky^{†, 97} I. Szanyi^{†, 29, 28}
J. Sziklai^{‡, 29} C. Taylor^{†, 88} E. Tcherniaev^{†, 53} M. Titov^{†, 19} V.V. Tokmenin^{†, 47} Y.-T. Tsai^{†, 85} D. Tsybychev^{†, 86}
B. Tuchming^{†, 19} C. Tully^{†, 83} N. Turini^{‡, 41} O. Urban^{†, 7} L. Uvarov^{†, 52} S. Uvarov^{†, 52} S. Uzunyan^{†, 69} V. Vacek^{†, 9}
R. Van Kooten^{†, 71} W.M. van Leeuwen^{†, 44} N. Varelas^{†, 68} E.W. Varnes^{†, 63} I.A. Vasilyev^{†, 51} O. Vavroch^{†, 7}
A.Y. Verkheev^{†, 47} L.S. Vertogradov^{†, 47} M. Verzocchi^{†, 67} M. Vesterinen^{†, 62} D. Vilanova^{†, 19} P. Vokac^{†, 9}
H.D. Wahl^{†, 66} C. Wang^{†, 5} M.H.L.S. Wang^{†, 67} J. Warchol^{‡, 73} G. Watts^{†, 98} M. Wayne^{†, 73} J. Weichert^{†, 25}
J. Welti^{†, 12, 13} L. Welty-Rieger^{†, 70} J. Williams^{‡, 75} M.R.J. Williams^{n†, 71} G.W. Wilson^{†, 75} M. Wobisch^{†, 76}
D.R. Wood^{†, 77} T.R. Wyatt^{†, 62} Y. Xie^{†, 67} R. Yamada^{†, 67} S. Yang^{†, 5} T. Yasuda^{†, 67} Y.A. Yatsunenko^{‡, 47}
W. Ye^{†, 86} Z. Ye^{†, 67} H. Yin^{†, 67} K. Yip^{†, 87} S.W. Youn^{†, 67} J.M. Yu^{†, 78} J. Zennaro^{†, 84} T.G. Zhao^{†, 62}
B. Zhou^{†, 78} J. Zhu^{†, 78} J. Zich^{‡, 7} K. Zielinski^{‡, 46} M. Zielinski^{†, 85} D. Zieminska^{†, 71} and L. Zivkovic^{p†18}

(D0[†] and TOTEM[‡] Collaborations*)

¹LAFEX, Centro Brasileiro de Pesquisas Físicas, Rio de Janeiro, RJ 22290, Brazil

²Universidade do Estado do Rio de Janeiro, Rio de Janeiro, RJ 20550, Brazil

³Universidade Federal do ABC, Santo André, SP 09210, Brazil

⁴INRNE-BAS, Institute for Nuclear Research and Nuclear Energy, Bulgarian Academy of Sciences, Sofia, Bulgaria

⁵University of Science and Technology of China, Hefei 230026, People's Republic of China

⁶Universidad de los Andes, Bogotá, 111711, Colombia

⁷University of West Bohemia, Pilsen, Czech Republic

⁸Charles University, Faculty of Mathematics and Physics,
Center for Particle Physics, 116 36 Prague 1, Czech Republic

⁹Czech Technical University in Prague, 116 36 Prague 6, Czech Republic

¹⁰Institute of Physics, Academy of Sciences of the Czech Republic, 182 21 Prague, Czech Republic

¹¹Universidad San Francisco de Quito, Quito 170157, Ecuador

¹²Helsinki Institute of Physics, University of Helsinki, Helsinki, Finland

¹³Department of Physics, University of Helsinki, Helsinki, Finland

¹⁴LPC, Université Blaise Pascal, CNRS/IN2P3, Clermont, F-63178 Aubière Cedex, France

¹⁵LPSC, Université Joseph Fourier Grenoble 1, CNRS/IN2P3,
Institut National Polytechnique de Grenoble, F-38026 Grenoble Cedex, France

¹⁶CPPM, Aix-Marseille Université, CNRS/IN2P3, F-13288 Marseille Cedex 09, France

¹⁷LAL, Univ. Paris-Sud, CNRS/IN2P3, Université Paris-Saclay, F-91898 Orsay Cedex, France

¹⁸LPNHE, Universités Paris VI and VII, CNRS/IN2P3, F-75005 Paris, France

¹⁹IRFU, CEA, Université Paris-Saclay, F-91191 Gif-Sur-Yvette, France

²⁰IPHC, Université de Strasbourg, CNRS/IN2P3, F-67037 Strasbourg, France

²¹IPNL, Université Lyon 1, CNRS/IN2P3, F-69622 Villeurbanne Cedex,
France and Université de Lyon, F-69361 Lyon CEDEX 07, France

²²III. Physikalisches Institut A, RWTH Aachen University, 52056 Aachen, Germany

²³Physikalisches Institut, Universität Freiburg, 79085 Freiburg, Germany

²⁴II. Physikalisches Institut, Georg-August-Universität Göttingen, 37073 Göttingen, Germany

²⁵Institut für Physik, Universität Mainz, 55099 Mainz, Germany

²⁶Ludwig-Maximilians-Universität München, 80539 München, Germany

²⁷Department of Atomic Physics, ELTE University, Budapest, Hungary

²⁸Eötvös University, H - 1117 Budapest, Pázmány P. s. 1/A, Hungary

²⁹Wigner Research Centre for Physics, RMKI, Budapest, Hungary

³⁰SzIU KRC, Gyöngyös, Hungary

³¹Panjab University, Chandigarh 160014, India

³²Delhi University, Delhi-110 007, India

³³Tata Institute of Fundamental Research, Mumbai-400 005, India

³⁴University College Dublin, Dublin 4, Ireland

³⁵INFN Sezione di Bari, Bari, Italy

³⁶Dipartimento Interateneo di Fisica di Bari, Bari, Italy

- ³⁷*Dipartimento di Ingegneria Elettrica e dell'Informazione - Politecnico di Bari, Bari, Italy*
- ³⁸*INFN Sezione di Genova, Genova, Italy*
- ³⁹*Università degli Studi di Genova, Italy*
- ⁴⁰*INFN Sezione di Pisa, Pisa, Italy*
- ⁴¹*Università degli Studi di Siena and Gruppo Collegato INFN di Siena, Siena, Italy*
- ⁴²*Korea Detector Laboratory, Korea University, Seoul, 02841, Korea*
- ⁴³*CINVESTAV, Mexico City 07360, Mexico*
- ⁴⁴*Nikhef, Science Park, 1098 XG Amsterdam, the Netherlands*
- ⁴⁵*Radboud University Nijmegen, 6525 AJ Nijmegen, the Netherlands*
- ⁴⁶*AGH University of Science and Technology, Krakow, Poland*
- ⁴⁷*Joint Institute for Nuclear Research, Dubna 141980, Russia*
- ⁴⁸*Institute for Theoretical and Experimental Physics, Moscow 117259, Russia*
- ⁴⁹*Moscow State University, Moscow 119991, Russia*
- ⁵⁰*Ioffe Physical - Technical Institute of Russian Academy of Sciences, St. Petersburg, Russian Federation*
- ⁵¹*Institute for High Energy Physics, Protvino, Moscow region 142281, Russia*
- ⁵²*Petersburg Nuclear Physics Institute, St. Petersburg 188300, Russia*
- ⁵³*Tomsk State University, Tomsk, Russia*
- ⁵⁴*Institució Catalana de Recerca i Estudis Avançats (ICREA) and Institut de Física d'Altes Energies (IFAE), 08193 Bellaterra (Barcelona), Spain*
- ⁵⁵*Department of Astronomy and Theoretical Physics, Lund University, SE-223 62 Lund, Sweden*
- ⁵⁶*Uppsala University, 751 05 Uppsala, Sweden*
- ⁵⁷*CERN, Geneva, Switzerland*
- ⁵⁸*Istanbul University, Istanbul, Turkey*
- ⁵⁹*Taras Shevchenko National University of Kyiv, Kiev, 01601, Ukraine*
- ⁶⁰*Lancaster University, Lancaster LA1 4YB, United Kingdom*
- ⁶¹*Imperial College London, London SW7 2AZ, United Kingdom*
- ⁶²*The University of Manchester, Manchester M13 9PL, United Kingdom*
- ⁶³*University of Arizona, Tucson, Arizona 85721, USA*
- ⁶⁴*University of California Riverside, Riverside, California 92521, USA*
- ⁶⁵*SLAC National Accelerator Laboratory, Stanford CA, USA*
- ⁶⁶*Florida State University, Tallahassee, Florida 32306, USA*
- ⁶⁷*Fermi National Accelerator Laboratory, Batavia, Illinois 60510, USA*
- ⁶⁸*University of Illinois at Chicago, Chicago, Illinois 60607, USA*
- ⁶⁹*Northern Illinois University, DeKalb, Illinois 60115, USA*
- ⁷⁰*Northwestern University, Evanston, Illinois 60208, USA*
- ⁷¹*Indiana University, Bloomington, Indiana 47405, USA*
- ⁷²*Purdue University Calumet, Hammond, Indiana 46323, USA*
- ⁷³*University of Notre Dame, Notre Dame, Indiana 46556, USA*
- ⁷⁴*Iowa State University, Ames, Iowa 50011, USA*
- ⁷⁵*University of Kansas, Lawrence, Kansas 66045, USA*
- ⁷⁶*Louisiana Tech University, Ruston, Louisiana 71272, USA*
- ⁷⁷*Northeastern University, Boston, Massachusetts 02115, USA*
- ⁷⁸*University of Michigan, Ann Arbor, Michigan 48109, USA*
- ⁷⁹*Michigan State University, East Lansing, Michigan 48824, USA*
- ⁸⁰*University of Mississippi, University, Mississippi 38677, USA*
- ⁸¹*University of Nebraska, Lincoln, Nebraska 68588, USA*
- ⁸²*Rutgers University, Piscataway, New Jersey 08855, USA*
- ⁸³*Princeton University, Princeton, New Jersey 08544, USA*
- ⁸⁴*State University of New York, Buffalo, New York 14260, USA*
- ⁸⁵*University of Rochester, Rochester, New York 14627, USA*
- ⁸⁶*State University of New York, Stony Brook, New York 11794, USA*
- ⁸⁷*Brookhaven National Laboratory, Upton, New York 11973, USA*
- ⁸⁸*Case Western Reserve University, Dept. of Physics, Cleveland, OH 44106, USA*
- ⁸⁹*Langston University, Langston, Oklahoma 73050, USA*
- ⁹⁰*University of Oklahoma, Norman, Oklahoma 73019, USA*
- ⁹¹*Oklahoma State University, Stillwater, Oklahoma 74078, USA*
- ⁹²*Oregon State University, Corvallis, Oregon 97331, USA*
- ⁹³*Brown University, Providence, Rhode Island 02912, USA*
- ⁹⁴*University of Texas, Arlington, Texas 76019, USA*
- ⁹⁵*Southern Methodist University, Dallas, Texas 75275, USA*
- ⁹⁶*Rice University, Houston, Texas 77005, USA*
- ⁹⁷*University of Virginia, Charlottesville, Virginia 22904, USA*
- ⁹⁸*University of Washington, Seattle, Washington 98195, USA*
- (Dated: December 9, 2020)

We describe an analysis comparing the $p\bar{p}$ elastic cross section as measured by the D0 Collaboration at a center-of-mass energy of 1.96 TeV to that in pp collisions as measured by the TOTEM Collaboration at 2.76, 7, 8, and 13 TeV using a model-independent approach. The TOTEM cross sections extrapolated to a center-of-mass energy of $\sqrt{s} = 1.96$ TeV are compared with the D0 measurement in the region of the diffractive minimum and the second maximum of the pp cross section. The two data sets disagree at the 3.4σ level and thus provide evidence for the t -channel exchange of a colorless, C -odd gluonic compound, also known as the odderon. We combine these results with a TOTEM analysis of the same C -odd exchange based on the total cross section and the ratio of the real to imaginary parts of the forward elastic scattering amplitude in pp scattering. The combined significance of these results is larger than 5σ and is interpreted as the first observation of the exchange of a colorless, C -odd gluonic compound.

PACS numbers: 13.60.Hb, 13.60.Fz, 13.85.Dz, 13.85.Lg, 12.38.-t, 12.38.Qk, 12.40.Nn

At high energies, the scattering amplitudes of both proton-proton (pp) and proton-antiproton ($p\bar{p}$) elastic collisions are dominated by t -channel exchanges that carry the quantum numbers of the vacuum. A charge (C) even and a subdominant C -odd combination can be formed from the pp and $p\bar{p}$ elastic scattering amplitude [1–5]. The differences between these cross sections are due to processes that involve the exchange of the odderon [1, 2], which couples differently to particles and their charge conjugates. In the quantum theory of strong interactions, quantum chromodynamics, this C -odd exchange is described by the t -channel exchange of a colorless three-gluon compound at leading order [6–8], where the binding strength among the gluons is greater than the strength of their interaction with other particles. At TeV energies the effects of t -channel virtual meson exchanges may be neglected [9].

The TOTEM Collaboration reported strong evidence that the measurements [10] of the ρ parameter, the ratio of the real to imaginary part of the forward elastic scattering amplitude, and the total cross section in pp scattering are inconsistent with the hypothesis of purely C -even exchanges for a range of models [11]. In this paper, we present independent evidence for C -odd exchanges based on a comparison of the pp and $p\bar{p}$ elastic scattering cross sections as a function of momentum transfer t , and combine the two measurements.

The D0 experiment [12] collected elastic $p\bar{p}$ data [13] at a center-of-mass energy \sqrt{s} of 1.96 TeV using special Tevatron optics and beams containing only one proton and one anti-proton bunch. About two million elastic events were collected in two separate data collection periods. The scattered p and \bar{p} were measured in the forward proton detectors (FPD). The FPD consisted of sets of scintillating fiber detectors downstream of the interaction point (IP) along the proton and anti-proton beam lines. The momenta of the scattered p and \bar{p} were measured in two stations of fibers located at distances of 23 and 31 m from the IP. The resolution for the measurement of the squared transverse momentum $|t|$ varied from 0.02 GeV² at $|t| \approx 0.25$ GeV² value to 0.04 GeV² at $|t| \approx 1.2$ GeV². The systematic uncertainties in the D0 results included the effects of the beam divergence, the uncertainty in the FPD positions, the choice of the Monte Carlo (MC) ansatz function used to calculate the acceptance, and the efficiencies of the scintillating fibers [13].

The TOTEM Collaboration at the CERN Large Hadron Collider (LHC) measured the differential elastic pp cross sections at $\sqrt{s} = 2.76$ [14], 7 [15], 8 [16] and 13 [17] TeV. The TOTEM experiment [18] utilizes sets of Roman Pot detectors (RPs) to detect elastically and diffractively scattered protons at very small angles. The RP system is composed of two arms placed symmetrically about interaction point 5 of the LHC. Each arm contains several RP stations between 213 m and 220 m from the IP. The detectors and their configurations were changed for the measurements at the different energies, but each measurement was based on a pair of RPs with a lever arm between 5 and 7 m. There are three RPs in each station, one approaching the beam from the top, one from the bottom, and one horizontally. Each RP is equipped with a stack of 10 silicon strip detectors designed with the objective of reducing the insensitive area at the edge facing the beam to only a few tens of micrometers. In each detector, the 512 strips with 66 μm pitch are oriented at an angle of $+45^\circ$ (five planes) and -45° (five planes) with respect to the detector edge facing the beam.

Figure 1 shows the D0 and TOTEM differential cross sections used in this study as functions of $|t|$ [19]. All pp cross sections show a common pattern of a diffractive minimum (“dip”) followed by a secondary maximum (“bump”) in $d\sigma/dt$. Fig. 2 shows the ratio R of the differ-

*with visitors from ^aAugustana University, Sioux Falls, SD 57197, USA, ^bThe University of Liverpool, Liverpool L69 3BX, UK, ^cDeutsches Elektronen-Synchrotron (DESY), Notkestrasse 85, Germany, ^dCONACyT, M-03940 Mexico City, Mexico, ^eSLAC, Menlo Park, CA 94025, USA, ^fUniversity College London, London WC1E 6BT, UK, ^gCentro de Investigacion en Computacion - IPN, CP 07738 Mexico City, Mexico, ^hUniversidade Estadual Paulista, São Paulo, SP 01140, Brazil, ⁱKarlsruher Institut für Technologie (KIT) - Steinbuch Centre for Computing (SCC), D-76128 Karlsruhe, Germany, ^jOffice of Science, U.S. Department of Energy, Washington, D.C. 20585, USA, ^kKiev Institute for Nuclear Research (KINR), Kyiv 03680, Ukraine, ^mUniversity of Maryland, College Park, MD 20742, USA, ⁿEuropean Organization for Nuclear Research (CERN), CH-1211 Geneva, Switzerland, ^oPurdue University, West Lafayette, IN 47907, USA, ^pInstitute of Physics, Belgrade, Belgrade, Serbia, and ^qP.N. Lebedev Physical Institute of the Russian Academy of Sciences, 119991, Moscow, Russia. [§]Deceased.

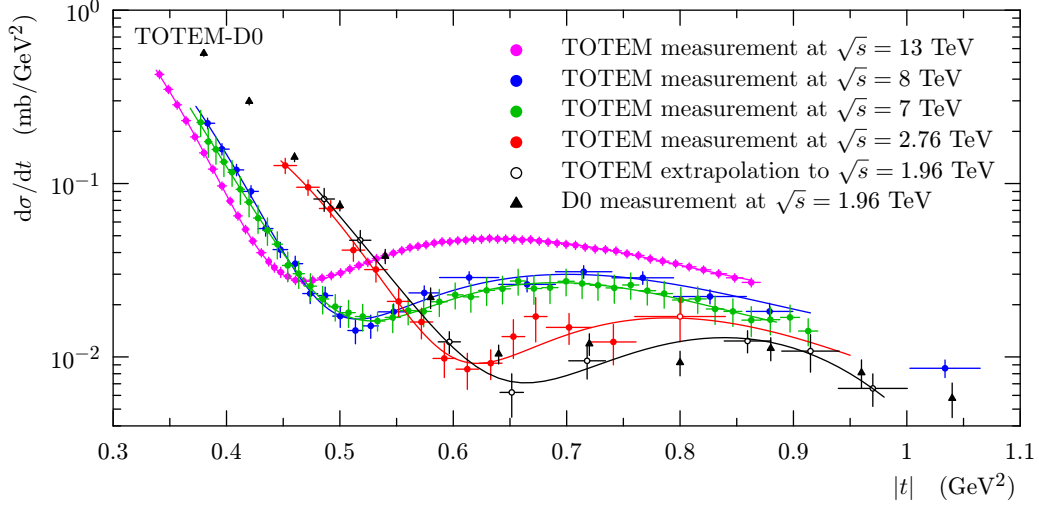


FIG. 1: The measured pp elastic cross sections as functions of $|t|$ at 2.76, 7, 8, and 13 TeV (full circles), and the extrapolation (discussed in the text) to 1.96 TeV (empty circles). The lines show the double exponential fits to the TOTEM data (see text). The $p\bar{p}$ measurement by the D0 Collaboration at 1.96 TeV is also shown in full triangles.

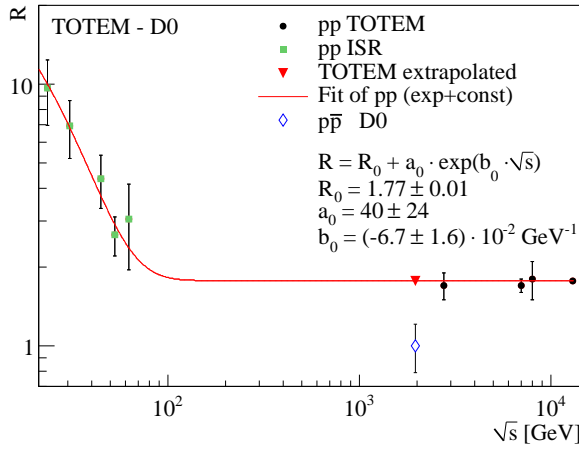


FIG. 2: The ratio, R , of the cross sections at the bump and dip as a function of \sqrt{s} . The points for $\sqrt{s} < 100$ GeV are from the ISR measurements. The pp data are fitted to the function noted in the legend. The ratio for the D0 $p\bar{p}$ results is shown at $\sqrt{s} = 1.96$ TeV.

ential cross sections measured at the bump and dip locations as a function of \sqrt{s} for ISR [20] and TOTEM [14–17] pp elastic cross section data. The pp data are fitted using the formula $R = R_0 + a_0 \exp(b_0 \sqrt{s})$. We note that R decreases as a function of \sqrt{s} in the ISR regime and flattens out at LHC energies. Since there is no discernible dip or bump in the $p\bar{p}$ cross section, we estimate R by taking the maximum ratio of the measured $d\sigma/dt$ values over the three neighboring bins centered on the bump and dip locations predicted by the TOTEM measurements. The $p\bar{p}$ value, $R = 1.0 \pm 0.2$, differs from the pp ratio by more than 3σ assuming that the flat R behavior of the pp cross

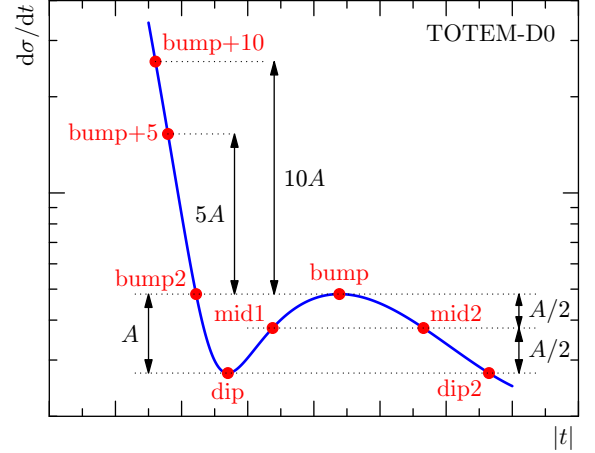


FIG. 3: Schematic definition of the characteristic points in the TOTEM differential cross section data. A represents the vertical distance between bump and dip.

section ratio at the LHC continues down to 2 TeV.

Motivated by the features of the pp elastic $d\sigma/dt$ measurements, we define a set of eight characteristic points, as shown in Fig. 3. For each characteristic point, we identify the values of $|t|$ and $d\sigma/dt$ at the closest measured points to the characteristic point, thus avoiding the use of model-dependent fits. In cases where two adjacent points are of about equal value, the data bins are merged. This leads to a distribution of $|t|$ and $d\sigma/dt$ values as a function of \sqrt{s} for all characteristic points as shown in Fig. 4. The uncertainties correspond to half the bin size in $|t|$ (comparable to the $|t|$ -resolution) and to the published uncertainties on the cross sections.

The values of $|t|$ and $d\sigma/dt$ as functions of \sqrt{s} for each

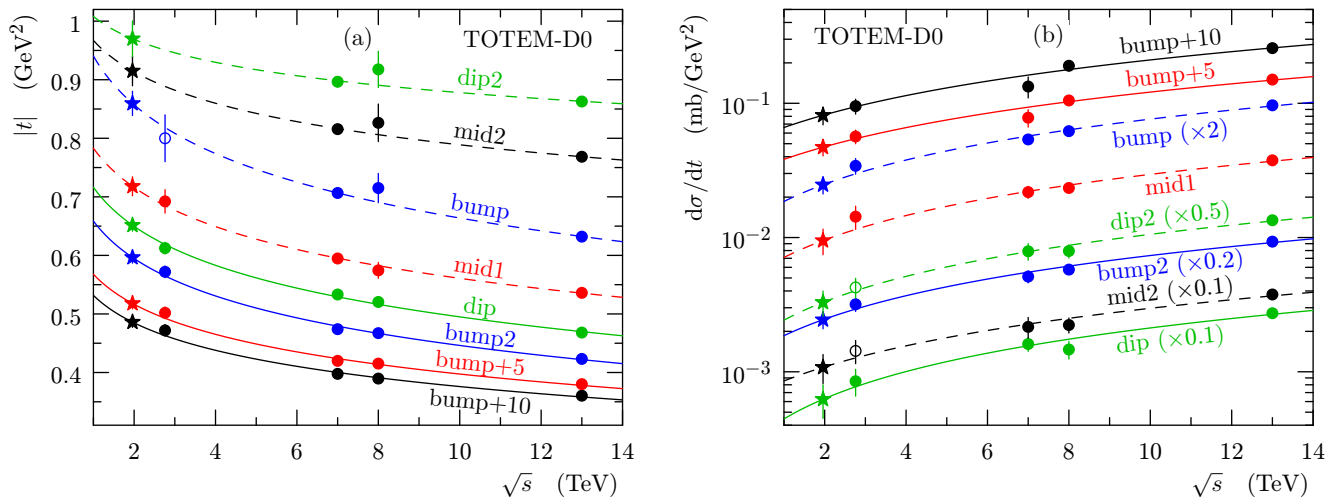


FIG. 4: Characteristic points in (a) $|t|$ and (b) $d\sigma/dt$ from TOTEM measurements at 2.76, 7, 8, and 13 TeV (circles) as a function of \sqrt{s} extrapolated to Tevatron center-of-mass energy (stars) using (a) Eq. 1 and (b) Eq. 2. On (b), a multiplication factor indicated in parenthesis is applied in order to distinguish the different fits. Filled symbols are from measured points; open symbols are from extrapolations or definitions of the characteristic points.

characteristic point are fitted using the functional forms

$$|t| = a \log(\sqrt{s}) + b \quad (1)$$

$$(d\sigma/dt) = c\sqrt{s} + d. \quad (2)$$

The parameter values are determined for each characteristic point separately and the same functional form describes the dependence for all characteristic points. The fact that the same form can be used for all points is not obvious and might be related to general properties of elastic scattering [21]. The χ^2 values for the majority of fits are close to 1 per degree of freedom (dof). Alternative forms that give adequate fits yield extrapolated values that are the same within uncertainties, hence the approach used is essentially model-independent.

The $|t|$ and $d\sigma/dt$ values extrapolated for the characteristic points for pp interactions at 1.96 TeV are displayed as open black circles in Fig. 1. The uncertainties on the extrapolated $|t|$ and $d\sigma/dt$ values are computed using a full treatment of the fit uncertainties, taking into account the fact that the systematic uncertainties of the different characteristic points are not correlated because they correspond to different data sets and running conditions.

To compare the extrapolated pp elastic cross sections with the $p\bar{p}$ measurements, we compute the pp cross sections at the same $|t|$ -values as in the D0 measurements (in the interval $0.50 \leq |t| \leq 0.96$ GeV²). We fit the pp extrapolated data at 1.96 TeV with the function

$$h(t) = a_1 e^{-a_2 |t|^2 - a_3 |t|} + a_4 e^{-a_5 |t|^3 - a_6 |t|^2 - a_7 |t|}. \quad (3)$$

The fit gives a χ^2 of 0.63 per dof [22]. The first exponential in Eq. (3) describes the cross section up to the location of the dip, where it falls below the second exponential that describes the asymmetric bump and subsequent falloff. This functional form (with non-zero a_7)

also provides a good fit for the measured pp cross sections at all energies as shown by the fitted functions in Fig. 1.

We evaluate the pp extrapolation uncertainty from MC simulation in which the cross section values of the eight characteristic points are varied within their Gaussian uncertainties and the fits given by Eq. 3 are performed. Fits without a dip and bump position matching the extrapolated values within their uncertainties are rejected, and slope and intercept constraints are used to discard unphysical fits [23]. The MC simulation ensemble provides a Gaussian-distributed pp cross section at each t -value, allowing a 1σ uncertainty band to be defined. However, the dip and bump matching constraints cause the median of the band to deviate from the best-fit cross sections. For the χ^2 comparison with the D0 measurements below we choose to use the center of the band.

We scale the pp extrapolated cross section so that the optical point (OP), $d\sigma/dt(t=0)$, is the same as that for $p\bar{p}$. The cross sections at the OP are expected to be equal if there are only C -even exchanges. Possible C -odd effects [21] are taken into account below as systematic uncertainties. Rescaling the OP for the extrapolated pp cross section would not itself constrain the behavior away from $t=0$. However, as demonstrated in Refs. [24, 25] the ratio of the pp and $p\bar{p}$ integrated elastic cross sections becomes one in the limit $\sqrt{s} \rightarrow \infty$. The parts of the elastic cross sections in the low $|t|$ Coulomb-nuclear interference region and in the high $|t|$ region above the exponentially falling diffractive cone that do differ for pp and $p\bar{p}$ scattering contribute negligibly to the total elastic cross sections. Thus, to excellent approximation, the integrated pp and $p\bar{p}$ elastic cross sections in the exponential diffractive region should be the same, implying that the logarithmic slopes should be the same. As this is the case within uncertainty for the pp and $p\bar{p}$ cross sections

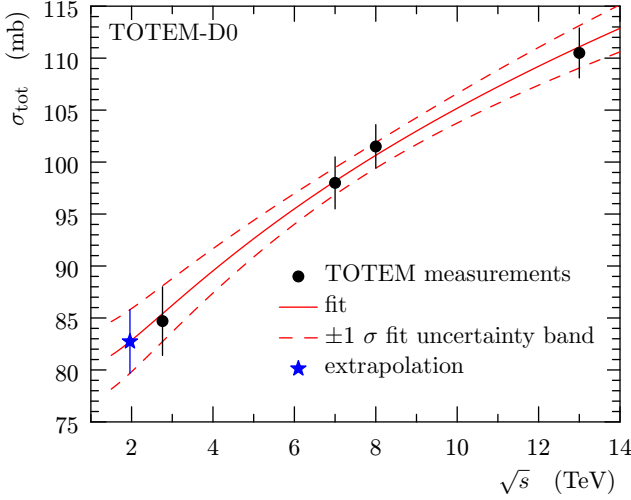


FIG. 5: Total cross section measurements by TOTEM at 2.76, 7, 8, and 13 TeV (black circles) extrapolated to 1.96 TeV (blue star). The dashed lines represent the 1σ uncertainty band.

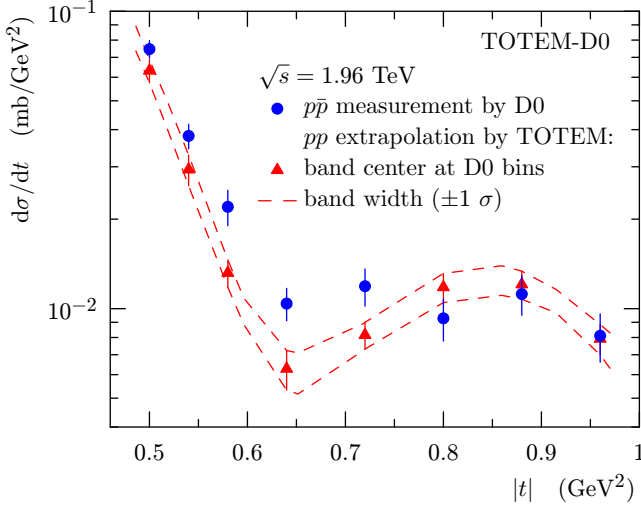


FIG. 6: Comparison between the D0 $p\bar{p}$ measurement at 1.96 TeV and the extrapolated TOTEM pp cross section, rescaled to match the OP of the D0 measurement. The dashed lines show the 1σ uncertainty band.

before the OP normalization, we choose to constrain the scaling to preserve the measured logarithmic slopes. We assume that no t -dependent scaling at t values beyond the diffractive cone ($|t| \geq 0.55$) is necessary.

To obtain the OP for pp at 1.96 TeV, we compute the total cross section by extrapolating the measurements by the TOTEM Collaboration at 2.76, 7, 8, and 13 TeV as illustrated in Fig. 5. A two-parameter fit of σ_{tot} is performed using

$$\sigma_{tot} = b_1 \log^2(\sqrt{s}/1\text{TeV}) + b_2 \quad (4)$$

with a $\chi^2 = 0.27$ for 2 dof, $b_1 = 4.63 \pm 0.72$ mb, and

$b_2 = 80.64 \pm 3.36$ mb, leading to an estimate of the total cross section at the Tevatron energy of $\sigma_{tot} = 82.7 \pm 3.1$ mb. The extrapolated cross section is converted to a differential cross section $d\sigma/dt = 357 \pm 26$ mb/GeV² at $t = 0$ using the optical theorem

$$\sigma_{tot}^2 = \frac{16\pi(\hbar c)^2}{1 + \rho^2} \left(\frac{d\sigma}{dt}(t=0) \right). \quad (5)$$

We assume $\rho = 0.145$ based on the COMPETE extrapolation [11]. The D0 Collaboration published an exponential fit of $d\sigma/dt$ in the range $0.26 < |t| < 0.6$ GeV² [13], which is extrapolated to $t = 0$ to give the OP cross section of 341 ± 48 mb/GeV². Thus the TOTEM OP and extrapolated $d\sigma/dt$ values are rescaled by 0.954 ± 0.071 (consistent with the OP uncertainties), where the uncertainty is due to that on the TOTEM extrapolated OP. We note that we do not claim that we have performed a measurement of $d\sigma/dt$ at the OP at $t = 0$ since this would require additional measurements of the elastic cross section closer to $t = 0$, but we require equal OPs simply to obtain a common and somewhat arbitrary normalization for the two data sets.

The assumption of the equality of the pp and $p\bar{p}$ elastic cross sections at the OP could be modified if an odderon exists [1, 2]. A reduction of the significance of a difference between pp and $p\bar{p}$ cross sections would only occur if the pp total cross section were larger than the $p\bar{p}$ total cross section at 1.96 TeV. This is the case only in maximal odderon scenarios [21], in which a 1.19 mb difference of the pp and $p\bar{p}$ total cross sections at 1.96 TeV would correspond to a 2.9% effect for the OP. This is taken as an additional systematic uncertainty and added in quadrature to the quoted OP uncertainty estimated from the TOTEM total cross section fit. The effect of additional (Reggeon) exchanges [9, 26, 27], different methods for extrapolation to the OP, and potential differences in ρ for pp and $p\bar{p}$ scattering are negligible compared with the uncertainties in the experimental normalization. The comparison between the extrapolated and rescaled TOTEM pp cross section at 1.96 TeV and the D0 $p\bar{p}$ measurement is shown in Fig. 6 over the interval $0.50 \leq |t| \leq 0.96$ GeV².

We perform a χ^2 test to examine the probability for the D0 and TOTEM differential elastic cross sections to agree. The test uses the difference of the integrated cross section in the examined $|t|$ -range with its fully correlated uncertainty, and the experimental and extrapolated points with their covariance matrices. The correlations for the D0 measurements at different t -values are small, but the correlations between the eight TOTEM extrapolated data points are large due to the fit using Eq. 3, particularly for neighboring points. Given the constraints on the OP normalization and logarithmic slopes of the elastic cross sections, the χ^2 test with six degrees of freedom yields the p -value of 0.00061, corresponding to a significance of 3.4σ .

We make a cross check of this result using an adaptation of the Kolmogorov-Smirnov test in which correlations in uncertainties are taken into account using simu-

lated data sets [28, 29]. This cross check, including the effect of the difference in the integrated cross section in the examined $|t|$ -range via the Stouffer method [30], gives a p -value for the agreement of the pp and $p\bar{p}$ cross sections that is equivalent to the χ^2 test.

We interpret this difference in the pp and $p\bar{p}$ elastic differential cross sections as evidence that two scattering amplitudes are present and that their relative sign differs for pp and $p\bar{p}$ scattering. These two processes are even and odd under crossing (or C -parity) respectively and are identified as pomeron and odderon exchanges [1, 2]. The dip in the elastic cross section is generally associated with the t -value where the pomeron-dominated imaginary part of the amplitude vanishes. Therefore the odderon, believed to constitute a significant fraction of the real part of the amplitude, is expected to play a large role at the dip. In agreement with predictions [21, 31], the pp cross section exhibits a deeper dip and stays below the $p\bar{p}$ cross section at least until the bump region.

We combine the present evidence using the Stouffer method with the independent evidence of the odderon found by the TOTEM Collaboration using the measurements of the ρ parameter and total cross section [10] in a completely different $|t|$ domain. For the model preferred by COMPETE [11], the TOTEM ρ measurement at 13 TeV provided a 4.6σ significance [32], leading to a total significance of 5.7σ for the t -channel exchange of a colorless C -odd gluonic compound when combined with the present result. The combined significance ranges from 5.2 to 5.7σ depending on the model [11, 31] when also including the model uncertainties.

In conclusion, we have compared the D0 $p\bar{p}$ elastic cross sections at 1.96 TeV and the TOTEM pp cross sections extrapolated to 1.96 TeV from measurements at 2.76, 7, 8, and 13 TeV using a model independent method [33]. The pp and $p\bar{p}$ cross sections differ with a significance of 3.4σ , and this stand-alone comparison provides evidence that a t -channel exchange of a colorless C -odd gluonic compound, i.e. an odderon, is needed to describe elastic scattering at high energies [21]. When combined with the result of Ref. [10], the significance is in the range 5.2 to 5.7σ and thus constitutes the first experimental observation of the odderon.

The TOTEM collaboration is grateful to the CERN beam optics development team for the design and the successful commissioning of the different special optics and to the LHC machine coordinators for scheduling the dedicated fills. We acknowledge the support from the collaborating institutions and also NSF (USA), the Mag-

nus Ehrnrooth Foundation (Finland), the Waldemar von Frenckell Foundation (Finland), the Academy of Finland, the Finnish Academy of Science and Letters (The Vilho Yrjö and Kalle Väisälä Fund), the Circles of Knowledge Club (Hungary), the NKFIH/OTKA grant K 133046 and the EFOP-3.6.1- 16-2016-00001 grants (Hungary). Individuals have received support from Nylands nation vid Helsingfors universitet (Finland), MSMT CR (the Czech Republic), the János Bolyai Research Scholarship of the Hungarian Academy of Sciences, the New National Excellence Program of the Hungarian Ministry of Human Capacities and the Polish Ministry of Science and Higher Education Grant No. MNiSW DIR/WK/2018/13.

The D0 Collaboration has prepared this document using the resources of the Fermi National Accelerator Laboratory (Fermilab), a U.S. Department of Energy, Office of Science, HEP User Facility. Fermilab is managed by Fermi Research Alliance, LLC (FRA), acting under Contract No. DE-AC02-07CH11359.

The D0 collaboration thanks the staffs at Fermilab and collaborating institutions, and acknowledges support from the Department of Energy and National Science Foundation (United States of America); Alternative Energies and Atomic Energy Commission and National Center for Scientific Research/National Institute of Nuclear and Particle Physics (France); Ministry of Education and Science of the Russian Federation, National Research Center “Kurchatov Institute” of the Russian Federation, and Russian Foundation for Basic Research (Russia); National Council for the Development of Science and Technology and Carlos Chagas Filho Foundation for the Support of Research in the State of Rio de Janeiro (Brazil); Department of Atomic Energy and Department of Science and Technology (India); Administrative Department of Science, Technology and Innovation (Colombia); National Council of Science and Technology (Mexico); National Research Foundation of Korea (Korea); Foundation for Fundamental Research on Matter (The Netherlands); Science and Technology Facilities Council and The Royal Society (United Kingdom); Ministry of Education, Youth and Sports (Czech Republic); Bundesministerium für Bildung und Forschung (Federal Ministry of Education and Research) and Deutsche Forschungsgemeinschaft (German Research Foundation) (Germany); Science Foundation Ireland (Ireland); Swedish Research Council (Sweden); China Academy of Sciences and National Natural Science Foundation of China (China); and Ministry of Education and Science of Ukraine (Ukraine).

-
- [1] L. Lukaszuk, B. Nicolescu, A Possible interpretation of pp rising total cross sections, *Lett. Nuovo Cim.* **8**, 405 (1973).
 - [2] P. Gauron, L. Lukaszuk, B. Nicolescu, Consistency of the maximal odderon approach with the QFT constraints, *Phys. Lett. B* **294**, 298 (1992).

- [3] S. Nussinov, Colored-Quark Version of Some Hadronic Puzzles, *Phys. Rev. Lett.* **34**, 1286 (1975).
- [4] S. Nussinov, Perturbative recipe for quark-gluon theories and some of its applications, *Phys. Rev. D* **14**, 246 (1976).
- [5] D. Joynson, E. Leader, B. Nicolescu, C. Lopez, Non-regge and hyper-regge effects in pion-nucleon charge exchange

- scattering at high energies, *Nuovo Cim. A* **30**, 345 (1975).
- [6] E. Levin, M. Ryskin, High-energy hadron collisions in QCD, *Phys. Rep.* **189**, 268 (1990).
 - [7] M.A. Braun, Odderon and QCD, arXiv:hep-ph/9805394.
 - [8] V.A. Khoze, A.D. Martin, M.G. Ryskin, Elastic proton-proton scattering at 13 TeV, *Phys. Rev. D* **97**, 034019 (2018).
 - [9] L.V. Gribov, E.M. Levin and M. Ryskin, Semihard processes in QCD, *Phys. Rep.* **100**, 1 (1983).
 - [10] G. Antchev *et al.*, TOTEM Collaboration, First determination of the ρ parameter at $\sqrt{s}=13$ TeV – probing the existence of a colourless C-odd three-gluon compound state, *Eur. Phys. J. C* **79**, no.9, 785 (2019).
 - [11] J.R. Cudell *et al.*, COMPETE Collaboration, Benchmarks for the forward observables at RHIC, the Tevatron-run II and the LHC, *Phys. Rev. Lett.* **89**, 201801 (2020).
 - [12] V.M. Abazov *et al.*, D0 Collaboration, The upgraded D0 detector, *Nucl. Instrum. Methods A* **565** 463 (2006).
 - [13] V.M. Abazov *et al.*, D0 Collaboration, Measurement of the differential cross section $d\sigma/dt$ in elastic $p\bar{p}$ scattering at $\sqrt{s}=1.96$ TeV, *Phys. Rev. D* **86**, 012009 (2012).
 - [14] G. Antchev *et al.*, TOTEM Collaboration, Elastic differential cross-section $d\sigma/dt$ at $\sqrt{s}=2.76$ TeV and implications on the existence of a colourless C-odd three-gluon compound state, *Eur. Phys. J. C* **80**, no.2, 91 (2020).
 - [15] G. Antchev *et al.*, TOTEM Collaboration, Proton-proton elastic scattering at the LHC energy of $\sqrt{s}=7$ TeV, *EPL* **95**, no. 41004 (2011).
 - [16] G. Antchev *et al.*, TOTEM Collaboration, Evidence for non-exponential elastic pp differential cross-section at low $|t|$ and $\sqrt{s}=8$ TeV by TOTEM, *Nucl. Phys. B* **899**, 527 (2015).
 - [17] G. Antchev *et al.*, TOTEM Collaboration, Elastic differential cross-section measurement at $\sqrt{s}=13$ TeV by TOTEM, *Eur. Phys. J. C* **79**, no.10, 861 (2019).
 - [18] G. Antchev *et al.*, TOTEM Collaboration, Performance of the TOTEM detector at the LHC, *Int. J. Mod. Phys. A* **28**, 1330046 (2013).
 - [19] Full points are measured and open points are extrapolated.
 - [20] L. Baksay *et al.*, Measurement of the Proton Proton Total Cross-Section and Small Angle Elastic Scattering at ISR Energies, *Nucl. Phys. B* **148**, 538 (1979).
 - [21] E. Martynov, B. Nicolescu, Odderon effects in the differential cross-sections at Tevatron and LHC energies, *Eur. Phys. J. C* **79**, no.6, 461 (2019).
 - [22] The six parameters to fit the eight data points are $a_1 = 9.9 \text{ mb/GeV}^2$, $a_2 = 16.13 \text{ GeV}^{-4}$, $a_3 = 2.02 \text{ GeV}^{-2}$, $a_4 = 2.75 \times 10^{-6} \text{ mb/GeV}^2$, $a_5 = 28.57 \text{ GeV}^{-6}$, and $a_6 = -35.97 \text{ GeV}^{-4}$. The parameter a_7 was fixed to zero as it was not necessary to get a good data description.
 - [23] A few percent of the fits are discarded due to unphysical slopes deviating more than 10σ from the one reconstructed from the characteristic points. The number of fits discarded by the intercept constraint is negligible.
 - [24] I.I. Pomeranchuk, Equality of the nucleon and antinucleon total interaction cross section at high energies, *Zh. Eksp. Teor. Fiz.* **34**, no. 3, 725 (1958).
 - [25] H. Cornille, A. Martin, A “Pomeranchuk” theorem for elastic diffraction peaks, *Phys. Lett. B* **40B**, 671 (1972).
 - [26] W. Broniowski, L. Jenkovszky, E. R. Arriola, I. Szanyi, Hollowness in pp and $p\bar{p}$ scattering in a Regge model, *Phys. Rev. D* **98**, 074012 (2018).
 - [27] C. Royon, Recent results from the TOTEM Collaboration at the LHC, Proceedings of the Workshop on Forward Physics and QCD at the LHC, the Future Electron Ion Collider and Cosmic Ray Physics (2020), doi:10.17161/1808.30727.
 - [28] A.L. Cholesky, Sur la résolution numérique des systèmes d’équations linéaires, Cours de l’Ecole Polytechnique, France (1910).
 - [29] R.A. Horn, C.R. Johnson, Matrix Analysis, edition 2, Cambridge University Press (2012).
 - [30] S.Bityokov *et al.*, Two approaches to combine significances, Proceedings of Science PoS(ACAT08)118 (2008).
 - [31] V.A. Khoze, A.D. Martin, M.G. Ryskin, Elastic and diffractive scattering at the LHC, *Phys. Lett. B* **748**, 192 (2018).
 - [32] Ref. [10] reports a 4.7σ difference between the favored model of Ref. [11] and the TOTEM measurements. This is reduced to 4.6σ when the model uncertainties are taken into account.
 - [33] The model dependence is limited to the choice of function for fitting the extrapolated pp cross section (Eq. 3) and the use of existing models to estimate the systematic uncertainty due to the range of possible odderon contribution to the OP difference between pp and $p\bar{p}$.